Laboratory simulation of fluid-driven seismic sequences in shallow crustal conditions

Wai-lai Ying,[1] Philip M. Benson,[1] and R. Paul Young[1]

Received 28 July 2009; revised 2 September 2009; accepted 16 September 2009; published 16 October 2009.

[1] We report new laboratory simulations of fluid-induced seismicity on pre-existing faults in sandstone. By introducing pore pressure oscillations, faults were activated or reactivated to generate seismic sequences. These sequences were analysed using a slip-forecast model. Furthermore, field data from the Monticello reservoir was used to verify the model. Our results suggest that short-term forecasting is reliant upon the final stages when crack communication begins, limiting reservoir-induced seismicity (RIS) forecasting strategies to short periods. In addition, our laboratory data confirms the general accuracy and robustness of short-term forecast techniques dealing with natural crack-linkage processes, whether strain driven or fluid driven, ranging from volcanic hazard mitigation to episodic tremors and slips. Finally, oscillating pore pressure can prolong the period of fluid-induced seismicity, and the aftershock decay rate is slower than that without oscillations. **Citation:** Ying, W., P. M. Benson, and R. P. Young (2009), Laboratory simulation of fluid-driven seismic sequences in shallow crustal conditions, *Geophys. Res. Lett.*, *36*, L20301, doi:10.1029/2009GL040230.

1. Introduction

[2] Fluids are ubiquitous in the Earth's crust and are of prime importance in processes such as stress rotation [*Faulkner et al.*, 2006; *Fitzenz and Miller*, 2004], high pressure pulse induced aftershocks [*Miller et al.*, 2004], and the generation of seismic swarms [*Yamashita*, 1999; *Kilburn*, 2003; *Benson et al.*, 2008]. In addition, the importance of understanding pore fluid driven mechanisms is gaining significance in the engineered environment, for example, the influence of reservoir impoundment in the generation of local seismicity [*Gupta*, 1992, 2002, 2005; *Talwani*, 2000]. Although the role of pore fluids in fundamental crustal processes is well known, the precise relationship between pore fluid pressure and the mechanics of faulting in shallow crustal conditions remains not fully understood, because direct measurement of pore pressures in situ is not possible. In order to address some of these limitations, recent analyses have focused on fluid-induced micro-seismicity [*Benson et al.*, 2008; *Miyazawa et al.*, 2008] and aseismic fault movement [*Rubinstein et al.*, 2007; *Rogers and Dragert*, 2003], with the aim of establishing a relationship between fault nucleation and slip, and observable foreshock sequences [*Lin*, 2009; *Umino et al.*, 2002]. In some cases, the cyclical pressurisation of pre-existing faults due to seasonal and tidal changes may generate a transient stress resulting in measurable seismic sequences [*Rubinstein et al.*, 2007; *Richardson and Marone*, 2008]. In the shallow crust, the same effect is often seen as a result of the engineered environment, in particular the impoundment and discharge of surface reservoirs [*Gupta*, 1992, 2002; *Talwani*, 2000].

[3] Although the shallow crustal environment is under less overall stress than, for example, a deep subduction zone, the damage from earthquakes in these regions can be considerable due to their shallow focus. Several such earthquakes have occurred due to the impoundment of large dams, such as the M 6.3 event at the Koyna reservoir (India) and numerous earthquakes swarms at the Aswan reservoir (Eygpt). In order to better explain how pore fluids trigger seismicity, more data is required, not only to address hazard mitigation issues in the engineered environment, but also to investigate fundamental studies of tectonic earthquake triggering processes.

2. Methods

[4] Two sandstones were chosen for the experiments based on their initial porosity. Low porosity (~4%) Fontainebleau sandstone (FS) was compared to higher porosity (~13%) Darley Dale sandstone (DDS), with the aim of investigating the sequence of pore fluid driven seismicity, which is influenced by the hydrological properties of the rock. Right cylindrical samples of 50 mm diameter by 125 mm length were prepared. Triaxial deformation experiments were performed using a vessel equipped with 18 piezoelectric sensors for laboratory seismicity (known as acoustic emission, AE) detection, consisting of six sensors embedded in the steel loading platens and twelve in the rubber jacket. Pore pressure was independently controlled at each end of the sample via two intensifiers. Each intensifier was equipped with an advanced, digital servo-controller in order to generate a sinusoidal, cyclic, pressure variation. Pore pressure cycles were controlled from the bottom platen (upstream port) and monitored via a downstream port located in the top platen. Each experiment proceeded in three stages. In stage 1, faults were generated by loading the sample under constant strain rate (2×10^{-6} s^{-1}), constant confining pressure (20 MPa, ~0.8 km depth to simulate shallow crustal condition), and constant pore pressure (5 MPa) until failure. In stage 2, the strain rate was paused and pore pressure lowered to 2.5 MPa. This step locks the fault by increasing the effective pressure, allowing AE quiescence for stage 3. In this final stage, the fault was activated and reactivated via the cyclical pore pressure variations to induce seismicity (AE) along the pre-existing fractures. Different amplitudes of sinusoidal cyclic pore pressures were used for the study of initial seismicity, fault reactivation and protracted seismicity.

[1] Lassonde Institute, University of Toronto, Toronto, Ontario, Canada.

0094-8276/09/2009GL040230$05.00

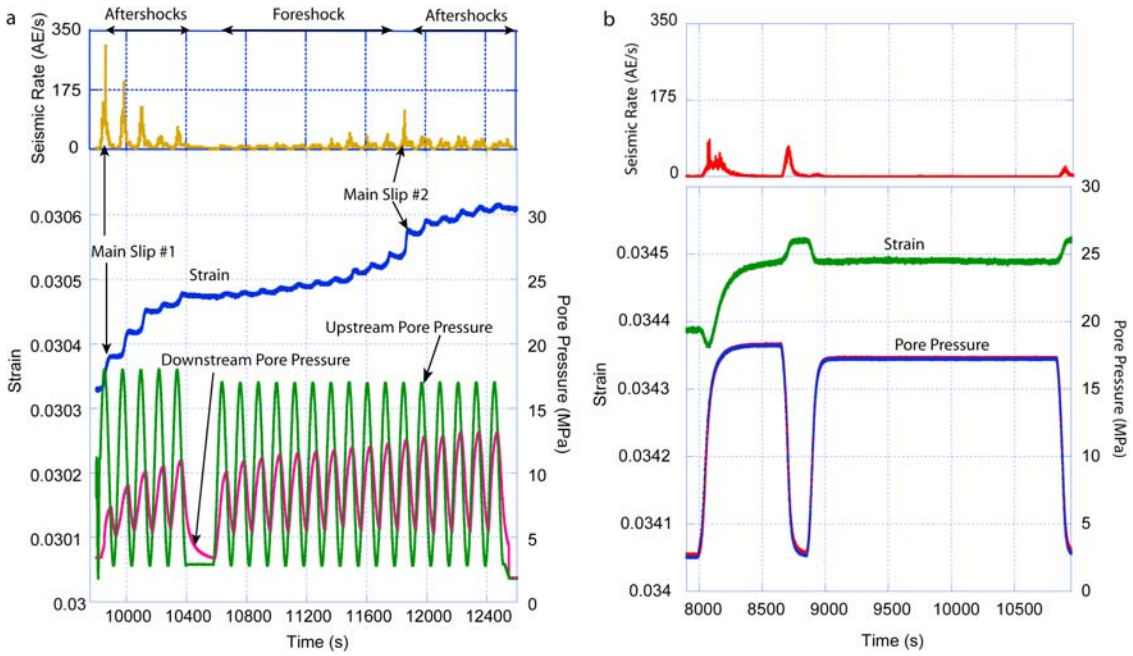

Figure 1. (a) Induced seismicity due to applied oscillatory pore pressures in FS. The downstream pore pressure cycles exhibited phase shifts and remained mostly transient in response to the upstream pore pressure cycles due to the relatively low porosity and heterogeneity of the fractured sample. The initial oscillation of upstream pore pressure between 18 and 2.5 MPa induced the main slip 1 due to the significant increase in pore pressure. Pore pressure was then reduced to 2.5 MPa to lock the fault. Subsequently the upstream pore pressure oscillated between 17 and 2.5 MPa. The foreshock sequence developed into the main slip 2, marked by significant strain change and a microseismic swarm, then followed by aftershock sequence. (b) The control experiment used pore pressure steps at 18 MPa for 10 minutes and 17 MPa for 32 minutes. The duration of seismicity is shorter, and the aftershock decay rate is much faster than that of the FS experiment.

For the FS experiment, we applied pore pressure oscillation ranging between 2.5 and 18 MPa to simulate activation of fault (or initial seismicity), and subsequently applied pore pressure oscillation ranging between 2.5 and 17 MPa (~95% of previous peak) to simulate fault reactivation and protracted seismicity. For the DDS experiment, several sets of fault activation were simulated using a range of pore pressure oscillations (Figure 2). In the Fontainebleau sandstone control experiment, all procedures in stage 1 and 2 remained unchanged (Figure 1). However, constant pore pressure steps were applied during stage 3. To permit direct comparison to the previous experiments, pore pressure steps at 18 MPa for 10 minutes and 17 MPa for 32 minutes were applied, which are equivalent to the duration of 5 cycles of aftershock sequences with peak pressure of 18 MPa, and 16 cycles of foreshock-aftershock sequences with peak pressure of 17 MPa, respectively. Seismic responses were recorded by a full waveform AE recorder (ASC Richter system), sampling at 10 MHz directly to hard disk storage for later processing of spatial and temporal distribution of seismic events.

3. Results

[5] For FS, a nearly instantaneous slip on the fracture plane was recorded when the average pore pressure was increased to higher than the previous maximum. Peak seismic rate occurred a few seconds after the applied peak pore pressure was reached, with aftershocks decay according to the Omori law [*Utsu*, 1961] with a p-value of 0.0039. This is a slower rate as compared to tectonic events, but is consistent with the RIS cases [*Gupta et al.*, 1972; *Gupta*, 2005]. Fault reactivation during the subsequent cycles is identified by a significant strain increase (main slip 2), accompanied by a microseismic swarm (Figure 1a). The number of pore pressure cycles required for reactivation is likely to be controlled by the hydrological properties of the fractured sample, which in turn determines the temporal development of pore pressure within the system. Key to this evolution is the connected porosity (permeability) of the fault network, which was measured before and after the experiments. Prior to pore pressure oscillation, a permeability of 5.7×10^{-17} m^2 was measured. Upon completion of the experiment, the permeability was 5.0×10^{-16} m^2, which is a significant increase.

[6] To confirm that the cyclical nature of pore pressure plays a key role in generating seismicity sequences, a control experiment on Fontainebleau sandstone was performed without sinusoidal pore pressure oscillations (Figure 1b). During the initial increase in pore pressure, the anticipated slip on the fault plane occurred, accompanied by a microseismic swarm with rate of decay (Omori p-value) of 0.0108 (approximately 2.8 times faster than that measured during the oscillating pore pressure stage). In addition, seismicity was also recorded during pore pressure reduction, which we attribute to the fault locking, and shearing of asperities within the damage zone. In the case of the control experiment, seismicity due to pore pressure increase is greatly reduced as compared to cyclical pore pressure (Figure 1). Finally, the pre-existing fault network in the control experiment could not be reactivated with a subsequent constant

Table 1. Cumulative Relative Axial Movement Along Fault As Inferred by Axial Strain Measurements

Period of Oscillation Pore Pressure	FS Cyclic Pore Pressure Experiment	Control Experiment
Peaks at 18 MPa	0.019 mm	0.019 mm
Peaks at 17 MPa	0.061 mm	0.006 mm

pore pressure reduction (i.e., at ~95% of previous maximum). This supports the hypothesis that cyclic pore pressure provides a key driving mechanism in shallow crustal fault zones, including those areas sensitive to RIS. Taken together, these observations confirm that the effect of oscillating pore pressure is to cause a longer period of seismicity (i.e., fault movement) than either a step increase in pore pressure or constant pressure alone. The majority of seismic events due to cyclic pressure occur over a longer period of time, whereas for step increases, seismicity reduced rapidly to its background level. The FS experiment also exhibits reactivation of fault and more substantial cumulative damage to the existing faults, as compared to the control experiment. These data are summarized in Table 1.

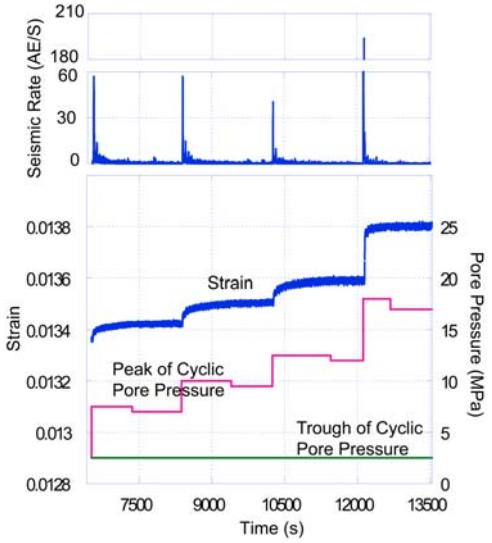

Figure 2. Induced seismicity due to oscillatory pore pressures in Daley Dale sandstone. A total of eight sets of pore pressure cycles were performed. These involve pore pressures cycled between a minimum of 2.5 MPa and a maximum of 7.5, 7.0, 10.0, 9.5, 12.5, 12.0, 18.0, and 17.0 MPa, respectively. The 7.5, 10.0, 12.5, and 18.0 MPa peak pore pressures sets simulates activation of fault, with increase in pore pressure exceeding the previous maximum. The 7.0, 9.5, 12.0, and 17.0 MPa pressure sets are at ~95% of the previous maximum, aiming to investigate reactivation of fault (Note: For clarity, only the peaks and troughs of the cyclic pore pressures are plotted for the sinusoidal pore pressure cycles). The upstream and downstream pore pressure are equilibrated instantaneously due to the high porosity of the sample. Significant strain change and seismicity were induced at each increase of pore pressure which exceeded the previous maximum. The pre-existing fault was not reactivated when peak pore pressures were lower than the previous maximum.

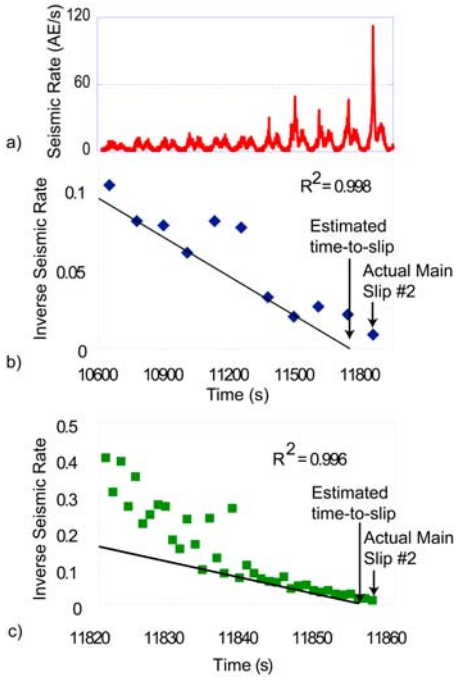

Figure 3. Application of a failure forecast model to experimental foreshock sequence obtained from FS experiment. (a) The seismic rate of the first 11 cycles during the foreshock sequence. (b) Long-term forecast using the peak seismic rate of each pore pressure cycles for the forecast of main slip 2. The estimated peak seismicity occurred in the 10th cycle, whilst the actual main slip occurred in the 11th cycle. (c) Short-term forecast using the seismic data of the 11th cycle. The estimated peak seismicity occurred at 11855 s, which is 2 s earlier than the actual occurrence (i.e., at 11857 s) of the peak seismicity.

[7] In contrast to FS data, DDS AE data shows a much faster response to the applied pressure cycles. Our results show that the existing fault was activated at each pore pressure increase exceeding the previous maximum attained, accompanied by significant strain change (Figure 2). Additionally, the aftershock sequence decay (Omori p-value of 0.158) indicates a faster decay rate than that of the FS. However, there was no fault reactivation when the pore pressure cycle peak values were reduced to ~95% of the previous maximum. The data indicates that hydraulic permeability (or diffusivity) is of key importance when assessing temporal evolution of RIS; this may also explain why so few locations have been identified as likely candidates for RIS, whether tectonic/tidal [*Richardson and Marone*, 2008; *Rubinstein et al.*, 2007] or shallow crustal/reservoir induced. In our experiments, DDS permits instantaneous equilibrium in pore pressure within the sample, while phase shifts and transient state of downstream pore pressure occurred in the lower porosity FS.

4. A Forecast Model for Pore-Fluid Induced Seismicity

[8] Although many earthquake prediction methods have been proposed in the past, these techniques have suffered from a lack of reliable data in the run-up to failure, i.e.,

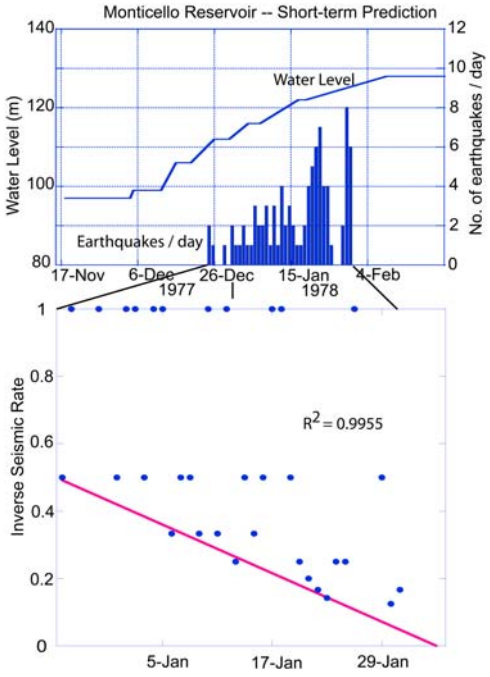

Figure 4. Short-term forecast for peak seismicity due to initial filling of Monticello reservoir [after *Chen and Talwani*, 2001]. Seismicity started about three weeks after the beginning of impoundment. The forecast model suggests the peak seismicity was on 6 February 1978, while the actual initial seismicity peaked in February 1978 [*Talwani*, 1997].

recording foreshock sequences, and how they can be identified as distinct from a regular shock before the event occurred [*Helmstetter and Sornette*, 2003]. However, in disciplines such as volcanology [*Kilburn*, 2003; *Lavallée et al.*, 2008], this is not a limitation as the repeated pressurisation of a volcanic edifice is cyclical in nature, as well as being governed by the same rock mechanical and physical processes as those which govern tectonic deformation. Thus, we adapt the failure forecast method of *Kilburn* [2003], which uses the concept that the time-to-failure or the occurrence of peak seismicity depends on the cumulative damage in weak zones. The acceleration in seismic frequency is described by [*Voight*, 1988, 1989; *Main*, 1999]:

$$\frac{d^2\Omega}{dt^2} = A\left(\frac{d\Omega}{dt}\right)^{\alpha} \tag{1}$$

where t is time, A is a constant, α is an exponent that measures the degree of non-linearity, typically $1 < \alpha < 2$ [*Kilburn*, 2003], and Ω is related to precursory strain. This equation is applied retrospectively to forecast failure. When approaching the final stages of ground deformation, crack growth becomes uncontrolled, and propagation is described by $\alpha = 2$. Thus, equation (1) can be re-written as:

$$\left(\frac{d\Omega}{dt}\right)^{-1} = \left(\frac{d\Omega}{dt}\right)_0^{-1} - A(t - t_0) \tag{2}$$

[9] A plot of inverse seismic rate against time follows a negative linear trend, so that the time at which the inverse rate is zero corresponds to the uncontrolled crack propagation. This specific time can be obtained by a linear extrapolation of the measured trend in the inverse seismic rate with time. When this analysis is applied to our laboratory AE data, the FS foreshock sequence shows a similar dependence of inverse foreshock seismicity with time (Figure 3). This is possible because laboratory AE has been well established as a scale invariant proxy for earthquakes [e.g., *Main*, 1999]. The estimated main slip (signified by substantial strain change) is forecast at cycle 10, a forecast error of approximately 10% as compared to the known slip time at cycle 11. Finally, to verify the forecast model, we applied this method to published field data of the Monticello reservoir (South Carolina, USA) (Figure 4), with a moving time window of 30 days. The result suggests that peak seismicity is expected on 6th February 1978, while the actual peak seismicity occurred in February 1978 [*Talwani*, 1997].

5. Conclusion

[10] We conclude that cyclic pore pressure provides a key driving mechanism in shallow crustal fault activation/reactivation and can prolong the period of seismicity. In addition, it gradually accumulates damage within the fault zone and reduces the aftershock decay rate. The heterogeneity and hydrological properties of the rock influence the prolonged transient state of pore pressure. Detailed surveillance of the upstream and downstream pore pressures can provide information about the pore pressure variation of local areas; while the simple forecast model can provide reasonable estimates of the time-to-failure based on episodes of seismicity in a manner analogous to volcanic hazard mitigation. However, it is likely that the draining of dams as a means to reduce seismic rate is not always possible within the short-term forecast period, owing to the delay in response of the downstream pore pressures.

[11] **Acknowledgments.** The triaxial deformation experiments were performed at the Rock Fracture Dynamics Laboratory at the University of Toronto, which is funded by a Natural Sciences and Engineering Research Council (NSERC) discovery grant and a Canadian Foundation for Innovation award to R.P.Y. P.M.B was partially supported by a Marie-Curie International Fellowship within the 6th European Community Framework program (contract MOIF-CT-2005-020167 to P.M.B).

References

Benson, P. M., S. Vinciguerra, P. G. Meredith, and R. P. Young (2008), Laboratory simulation of volcano seismicity, *Science*, *322*, 249–252, doi:10.1126/science.1161927.

Chen, L., and P. Talwani (2001), Mechanism of initial seismicity following impoundment of the Monticello reservoir, South Carolina, *Bull. Seismol. Soc. Am.*, *91*, 1582–1594, doi:10.1785/0120000293.

Faulkner, D. R., T. M. Mitchell, D. Healy, and M. J. Heap (2006), Slip on "weak" faults by the rotation of regional stress in the fracture damage zone, *Nature*, *444*, 922–925, doi:10.1038/nature05353.

Fitzenz, D. D., and S. A. Miller (2004), New insights on stress rotations from a forward regional model of the San Andreas fault system near its Big Bend in southern California, *J. Geophys. Res.*, *109*, B08404, doi:10.1029/2003JB002890.

Gupta, H. K. (1992), *Reservoir-Induced Earthquakes*, 364 pp., Elsevier, Amsterdam.

Gupta, H. K. (2002), A review of recent studies of triggered earthquakes by artificial water reservoirs with special emphasis on earthquake in Koyna, India, *Earth Sci. Rev.*, *58*, 279–310, doi:10.1016/S0012-8252(02)00063-6.

Gupta, H. K. (2005), Artificial water reservoir-triggered earthquakes with special emphasis at Koyna, *Curr. Sci.*, *88*, 1628–1631.

Gupta, H. K., B. K. Rastogi, and H. Narain (1972), Common features of the reservoir associated seismic activities, *Bull. Seismol. Soc. Am.*, *62*, 481–492.

Helmstetter, A., and D. Sornette (2003), Foreshocks explained by cascades of triggered seismicity, *J. Geophys. Res.*, *108*(B10), 2457, doi:10.1029/2003JB002409.

Kilburn, C. R. J. (2003), Multiscale fracturing as a key to forecasting volcanic eruptions, *J. Volcanol. Geotherm. Res.*, *125*, 271–289, doi:10.1016/S0377-0273(03)00117-3.

Lavallée, Y., P. G. Meredith, D. B. Dingwell, K.-U. Hess, J. Wassermann, B. Cordonnier, A. Gerik, and J. H. Kruhl (2008), Seismogenic lavas and explosive eruption forecasting, *Nature*, *453*, 507–510, doi:10.1038/nature06980.

Lin, C. H. (2009), Foreshock characteristics in Taiwan: Potential earthquake warning, *J. Asian Earth Sci.*, *34*, 655–662, doi:10.1016/j.jseaes.2008.09.006.

Main, I. G. (1999), Applicability of time-to-failure analysis to accelerated strain before earthquake and volcanic eruptions, *Geophys. J. Int.*, *139*, F1–F6, doi:10.1046/j.1365-246x.1999.00004.x.

Miller, S. A., C. Collettini, L. Chiaraluce, M. Cocco, M. Barchi, and B. J. P. Kaus (2004), Aftershocks driven by a high-pressure CO_2 source at depth, *Nature*, *427*, 724–747, doi:10.1038/nature02251.

Miyazawa, M., A. Venkataraman, R. Snieder, and M. A. Payne (2008), Analysis of microearthquake data at Cold Lake and its applications to reservoir monitoring, *Geophysics*, *73*, O15, doi:10.1190/1.2901199.

Richardson, E., and C. Marone (2008), What triggers tremor?, *Science*, *319*, 166–167, doi:10.1126/science.1152877.

Rogers, G., and H. Dragert (2003), Episodic tremor and slip on the Cascadia subduction zone: The chatter of silent slip, *Science*, *300*, 1942–1943, doi:10.1126/science.1084783.

Rubinstein, J. L., J. E. Vidale, J. Gomberg, P. Bodin, K. C. Creager, and S. D. Malone (2007), Non-volcanic tremor driven by large transient shear stresses, *Nature*, *448*, 579–582, doi:10.1038/nature06017.

Talwani, P. (1997), On the nature of reservoir-induced seismicity, *Pure Appl. Geophys.*, *150*, 473–492, doi:10.1007/s000240050089.

Talwani, P. (2000), Seismogenic properties of the crust inferred from recent studies of reservoir-induced seismicity: Application to Koyna, *Curr. Sci.*, *79*, 1327–1333.

Umino, N., T. Okada, and A. Hasegawa (2002), Foreshock and aftershock sequence of the 1998 *M* 5.0 Sendai, northeastern Japan, earthquake and its implications for earthquake nucleation, *Bull. Seismol. Soc. Am.*, *92*, 2465–2477, doi:10.1785/0120010140.

Utsu, T. (1961), A statistical study on the occurrence of aftershocks, *Geophys. Mag.*, *30*, 521–605.

Voight, B. (1988), A method for prediction of volcanic eruption, *Nature*, *332*, 125–130, doi:10.1038/332125a0.

Voight, B. (1989), A relation to describe rate-dependent material failure, *Science*, *243*, 200–203, doi:10.1126/science.243.4888.200.

Yamashita, T. (1999), Pore creation due to fault slip in a fluid-permeated fault zone and its effect on seismicity: Generation mechanism of earthquake swarm, *Pure Appl. Geophys.*, *155*, 625–647, doi:10.1007/s000240050280.

P. M. Benson, W. Ying, and R. P. Young, Lassonde Institute, University of Toronto, Toronto, ON M5S 3E3, Canada. (winnie.ying@utoronto.ca)